**Journal of Nuclear Medicine, published on November 17, 2022 as doi:10.2967/jnumed.122.264941**

# 3-time-point PET-analysis of FAPI-46 in a variety of cancers

Naeimi-M[1], Choyke-P[3], Dendl-K[1], Mori-Y[2], Staudinger-F[1], Watabe-T[4], Koerber-SA[5], Röhrich-M[1], Debus-J[5], Kratochwil-C[1], Haberkorn-U[1], Giesel-FL[1,2]

1. Department of Nuclear Medicine, University Hospital Heidelberg, Im Neuenheimer Feld 400, 69120, Heidelberg, Germany
2. Department of Nuclear Medicine, Medical Faculty of Heinrich Heine University, University Hospital Düsseldorf, Moorenstrasse 5, 40225 Düsseldorf
3. Molecular Imaging Branch, Center for Cancer Research, National Institutes of Health (NIH/NCI), MSC1088, Bethesda, Maryland 20892-1088, United States.
4. Department of Nuclear Medicine and Tracer Kinetics, Osaka University Graduate School of Medicine, 2-2 Yamadaoka, Suita, Osaka, 565-0871, Japan.
5. Department of Radiation Oncology, University Hospital Heidelberg, Im Neuenheimer Feld 400, 69120, Heidelberg, Germany

**Full name of authors:**

Mahnoosh Naeimi, Peter L. Choyke, MD, Katharina Dendl, Yuriko Mori, MD, Fabian Staudinger, MD, Tadashi Watabe, MD, Stefan A. Koerber, MD, Manuel Röhrich, MD, Jürgen Debus, MD, Clemens Kratochwil, MD, Uwe Haberkorn, MD, Frederik L. Giesel, MD, MBA

**First author:**

Mahnoosh Naeimi

Department of Nuclear Medicine, University Hospital Heidelberg, Im Neuenheimer Feld 400, Heidelberg, Germany. Tel: +49 (6221) 566998 Fax: +49 (6221) 565999

Email: mahnoosh.naeimi@gmail.com

Current status: Resident

**Corresponding author:**
Frederik L. Giesel, MD, MBA
Department of Nuclear Medicine, University Hospital Duesseldorf, Duesseldorf, Germany. Tel: +49 (0211) 81-18540 Fax: +49 (0211) 81-17041
Email: frederik.giesel@med.uni-duesseldorf.de

**Short title:** 3-time-point PET-analysis of FAPI-46

**Word count:** 2080 words

**Disclosure:**

U.H. and F.L.G. have filed a patent application for quinoline-based FAP- targeting agents for imaging and therapy in nuclear medicine. U.H. and F.L.G. also have shares in a consultancy group for iTheranostics. F.L.G. is advisor at ABX, Telix pharma and SOFIE Bioscience. No other potential conflict of interest relevant to this article exist.

**Acknowledgements:**

Highly appreciate the support of Peter Pätsch for data analysis.

**ABSTRACT:**

**Purpose:** A growing family of $^{68}$Ga-FAPI Positron Emission Tomography (PET) probes have shown promise in imaging a variety of medical conditions. $^{68}$Ga-FAPI-46 in particular has emerged as unique for both its diagnostic and theranostic applications, however the optimal timing of PET remains unclear. Therefore, we evaluated uptake values at three time points after FAP-46 administration in a spectrum of tumor types.

**Methods:** The cohort consisted of 43 patients with diverse cancer diagnoses undergoing $^{68}$Ga-FAPI-46-PET/CT at three time points (10 min, 1 h, 3 h). We determined the tracer uptake based on standardized uptake values (SUVmean and SUVmax) and tumor-to-background-ratios (TBR) (SUVmax/ SUVmean).

**Results:** There were 171 lesions in the 43 patients. Comparing all lesions at different time points, the mean SUVmax was maximal at 10 min (8.2) and declined slightly at 1h (8.15) and 3h (7.6) after tracer administration. Similarly, the mean SUVmax(log) still had a similar pattern in primary lesions (n=30; 0.98, 1.01, 0.98), lymph node metastases (n=37; 0.82, 0.84, 0.81) and distant metastases (n=104; 0.81, 0.79, 0.74). TBR also showed non-significant differences at the three times.

**Conclusion:** $^{68}$Ga-FAPI-46-PET/CT imaging revealed remarkably stable tumor and background uptake as determined by SUV-metrics and maintained high TBRs within 3 hours of injection. Thus, it may be possible to scan with FAPI-46 within 10 to 20 minutes of injection, improving workflow and decreasing patient wait times. Confirmation of these findings in a larger cohort is underway.

**Keywords:** FAPI; Fibroblast Activation Protein; PET; PET/CT; 3-time-point

## Introduction

Reliable staging tools are vital for oncologic management. Molecular imaging probes have been advancing rapidly and are capable of detecting cancer with high sensitivity. Fibroblast activation protein (FAP) is expressed by cancer-associated fibroblasts in many cancer types and is implicated in tumor cell migration, invasion, cell signaling and tumor angiogenesis (*1-3*). FAP therefore, represents an interesting target for new molecular imaging and therapeutic agents. The development of a quinoline-based FAP inhibitor (FAPI), with high affinity for FAP represents an opportunity to exploit this target for PET imaging (*4*). Such radiolabeled quinoline-based ligands have shown promising results in previous studies (*5-7*).

By convention most molecular imaging agents are scanned one hour after injection. Likewise for FAP imaging most of the previously published studies involve acquiring static PET images 1 hour post injection (*7*). However, there are conflicting reports in the literature about optimal incubation times for FAPI agents and no conclusive data has been published (*8-12*). In this investigation, we compared different incubation times of the agent $^{68}$Ga-FAPI-46 in different cancers at three time points, 10 min, 1 hour and 3 hours.

## Methods

### *Patient cohort*

This was a retrospective study of 43 patients with various malignancies who underwent $^{68}$Ga-FAPI-46-PET/CT. The tumor types are summarized in Table 1. All imaging was performed at one center and all patients were referred by their attending oncologist or radiation oncologist for one of three reasons: 1. improve delineation of target volume for radiotherapy planning 2. restaging with ambiguous findings on conventional imaging or 3. follow-up. All patients gave written informed

consent to undergo $^{68}$Ga-FAPI-PET/CT on an individual patient basis following national regulations and the declaration of Helsinki. The radiopharmaceutical was synthesized and labeled according to the German Pharmaceutical Act §13(2b). The data were analyzed retrospectively with approval of the local ethics committee (S016/2018).

***Radiopharmaceuticals and Ga-FAPI-PET/CT imaging***

FAPI-46 was synthetized and labelled as previously described (*13*). A non-contrast-enhanced low-dose-CT (130 keV, 30 mAs, CareDose; reconstructed with a soft-tissue kernel to a slice thickness of 5 mm) and a Biograph mCT Flow scanner (Siemens) were used for imaging. All PET scans were acquired in 3D mode (matrix 200x200). Each patient underwent PET/CT imaging scans at 3 time points after radiotracer injection: 10 min., 1 h, and 3 h. after the injection of the radiotracer. Patients were evaluated for adverse effects at several times during the examination and vital signs were monitored until 30 min after the end of the examination.

***Image evaluation***

The tracer uptake and biodistribution were quantified by SUVmax and SUVmean at 10 minutes, 1 hour and 3 hours post injection of FAPI-46. (Fig. 1). For SUV calculation, circular volumes of interest were drawn manually around tumor lesions on transaxial slices at 1 hour and automatically transferred to the images obtained at 10 minutes and 3 hours, using a 3-dimensional volume of interest (VOI) with e.soft software (Siemens) at a 60% isocontour. Evaluation of normal organs was conducted with a 1 cm diameter (for the small organs thyroid, parotid gland, myocardium, oral mucosa, spinal cord, ovary) or 2 cm diameter (brain, muscle, liver, pancreas, spleen, kidney, fat, aortic lumen content, lung, mamma, endometrium) spherical region of interest (ROI) placed completely inside the organ parenchyma. For quantification of image contrast, tumor-to-background ratios (TBRs) were calculated. The formula was calculated using the geometric mean

of the quotients of lesion (SUVmax) to background tissue (SUVmean). Liver tissue, oral mucosa, fat and gluteal muscle were chosen as background tissue. The $^{68}$Ga-FAPI-PET/CT scans were analyzed in consensus by a board- certified radiologist, a board-certified radiation oncologist and two board-certified nuclear medicine physicians.

***Statistics:***

Descriptive analyses of patients and their tumors were performed. For determination of SUVs, median, arithmetic mean, standard deviation and the logarithm of SUVs to minimize potential mistakes during arithmetic mean calculations were used. The SUVs/logSUVs values were distributed normally, therefore a 2- sided t-test with paired samples was used to compare FAPI-46 SUVs in primary cancer, lymph node metastasis and distant metastasis at the 3 time points. A p-value of >0.05 was defined as statistically significant. All statistical analyses were performed using Excel for Mac Version 16.16 (Microsoft, Redmond, Washington, USA).

## Results

***Study population***

Our data consisted of 43 patients with various malignancies, that are summarized in Table 1. Lesions consisted of primary cancers / tumor relapse (n=30), lymphatic metastases (n=37) and distant metastases (n=104). The following tumor entities were included: lung cancer (n=11), colorectal cancer (n=6), pancreatic cancer (n=5), anal cancer (n=4), adrenocortical carcinoma (n=3), head and neck cancer (n=3), sarcoma, breast cancer, ovarian cancer (n=2), bladder cancer, neuroblastoma, lymphoma, prostate cancer (n=1) (see Table 1).

***Biodistribution in normal organs***

The biodistribution of $^{68}$Ga-FAPI-46 in normal organs is shown in Fig. 1, with stable low background activity and a mean uptake of SUVmax at 3 time points (10 min, 1 h, 3 h), of 1.6, 1.3, 1.2 respectively and mean uptake of SUVmean of 1.2, 1.0, 0.9 respectively.

Biodistribution in normal organs decreased slightly from 10 min to 3 h time points, however no significant difference was observed for SUVmax uptake among all normal organs (10 min vs. 3 h; p= 5.5, n=806). The highest tracer uptake in normal organs was always obtained on the first (10 min) scan except for fat tissue. The overall highest uptake was observed in oral mucosa and thyroid tissue. Thus, within the oral mucosa the mean SUVmax was 2.7, 2.2, 1.6 at the 3 time points, while for thyroid tissue the mean SUVmax was 2.6, 1.9, 1.6 respectively. The lowest tracer uptake was in the brain where mean SUVmax was 0.1, 0.1, 0.1, respectively (*Fig. 1*).

***Tumor uptake***

There were 171 lesions detected. All lesions were detected at all time points. For primary lesions and local relapse (n=30) the mean SUVmax log was 0.98, 1.0, 0.98 at the 3 time points. For lymph node metastases (n=37) the mean SUVmax log was 0.82, 0.84, 0.80 at the 3 time points. For distant metastases (n=104) the SUVmax log was 0.81, 0.78, 0.74 at the 3 time points. No significant difference was seen. The analysis of primary lesions or local relapse showed no significant difference in SUVmax uptake at the 3 time points in two way comparisons (10 min vs 1 h, P=0.2) (10 min vs 3 h; P=0.98), (1 h vs 3 h; P=0.2). The analysis of lymph node metastases (n=37) showed increased tumor uptake at 1 h compared to the other 2 time points (10 min and 3 h) with a significant difference for the comparison between 1 h vs 3 h; P=0.02. There were no significant differences in SUVmax uptake at other time points (10 min vs 1 h; P=0.26), (10 min vs 3 h; P=0.66). The analysis of distant metastases showed significant decrease of tumor uptake through the time points (10 min, 1 h, 3 h). The highest tumor uptake was observed at 10 min (10

min vs 1 h; P=0.02), (10 min vs 3 h, P=3.05E-0.5), (1 h vs 3 h; P=1.27E-0.5) (*Figs.* 2-3). Two examples of patients with tumors with similar uptake on $^{68}$Ga-FAPI-46 scan in 3 time points (10 min, 1 h, 3 h) are shown in *Figs. 4-5.*

***Tumor to background ratios***

Most of the background tissues showed a decrease in SUVmax and SUVmean at longer incubation times with the exception of fat tissue which had low SUVmax values of 0.32, 0.44, 0.44 and brain parenchyma with SUVmax values of 0.09, 0.13, 0,1. As expected, the primary/local relapse lesions demonstrated excellent contrast with normal tissue which increased through the time points (10 min, 1 h, 3 h) except TBR versus fat tissue. Increased TBR can also be measured in lymph nodes and distant metastases except for tumor to fat ratios which slightly decrease (*Fig.6)*. High TBRs are seen in primary/local relapse lesions versus fat tissue even after 3 h.

***Quantifying FAPI-46 uptake in different types of tumors***

The highest average of SUVmax > 20 in FAPI-46 scans was observed in primary lesions. The highest SUVs were seen in esophageal cancer (SUVmax 27.5; 3 h) and primary bladder cancer (SUVmax 29.2; 3 h). The highest SUVmax among all lymph node metastases was observed in esophageal lymph node metastases (SUVmax 19.5; 3 h). Among the distant metastases breast cancer metastases demonstrated the highest SUVmax among the tumors scanned (SUVmax 15.7; 10 min) (*Fig.*7).

## Discussion

The aim of this study was to evaluate the optimal uptake time of FAPI-46 based on time points between 10 minutes to 3 hours post injection. The uptake of FAPI-46, as measured by SUVmax, was remarkably stable at all three time points although the 10 min time point generally had slightly higher SUVmax values. The detection rate of tumors was equal at all time points implying that a diagnostic study can be achieved by 10 minutes of injection which will have implications for patient throughput and decreased patient waiting times in the Nuclear Medicine Department. Our study showed similar results to a previous analysis of early FAPI-PET acquisition at 5 different time points regarding finding the best time point for diagnostic imaging earlier than 60 min (*14*). Although due to the similar detection rate between 10 min and 1 h p.i. and a slightly higher tumor uptake at the 10 min time point, we would recommend 10 to 20 min p.i as the best time point for diagnostic imaging acquisition instead of 30 to 40 min p.i. (*14*).

The steady uptake of FAPI-46 also has implications for its use as a targeted theranostic agent where high dose delivery will be achieved early and will be maintained over at least several hours (*17*). Meanwhile, background uptake, largely responsible for toxicity in targeted treatments, appears to clear rapidly over 3 hours resulting in high tumor to background ratios consistent with prior reports (*4, 13*).

FAPI-46 is one of many FAPI derivatives but appears to have several desirable features including high affinity for the target and biological stability (*13, 19*). FAPI-46 showed no significant washout on time points between 10 minutes and 3 hours in comparison to other FAPI derivatives such as FAPI-02 with 75% washout und FAPI-04 with 25% washout after 3 h post injection (*15*), which makes FAPI-46 more valuable. Whereas the above mentioned study (*15*) was limited due to limited patient cohort, all three FAPI derivatives had shown similar biodistribution und high TBR value between 10 min to 3 h.

FAPI-46 uptake was compared in primary lesions, lymph node metastases and distant metastases in a spectrum of cancer types. The logSUVmax decreased over time in all stages of disease and the TBR commensurately increased over the same time period due to background washout. The findings were consistent regardless of the stage of the cancer lesion. These findings confirm prior studies showing similar results in a variety of cancers (*8, 11, 16, 20, 21).* It is expected that there will be minor differences in different single institution studies due to differences in the composition of the patient cohort and different types of tumor. Hu et al found similar results using two related derivatives of FAPI, FAPI-42 and FAPI-04 (9).

The TBRs obtained in this study were based on various background tissues including muscle, oral mucosa and liver. In each case the TBR increased as expected through time. This finding is in line with similar previous studies (*11, 16)*. The highest TBR is seen with comparisons of the tumor to fat tissue resulting in very high values even up to 3 h p.i. The highly favorable TBR obtained with FAPI agents in general and FAPI-46 specifically stands in contrast to the highly variable TBR obtained with FDG-PET scans.

This study has several limitations. Due to the limited number of patients, no reliable comparisons among each tumor type was possible. False positive findings in non-tumorous lesions or inflammation e.g. in the pancreas, could have influenced the results since histologic validation was not possible for all lesions. However, all patients were known to have extensive cancer based on conventional imaging and it is highly likely that the majority of the lesions measured in this study were cancers.

## Conclusion:

In conclusion, we presented that FAPI-46 is a robust FAPI targeting molecule that is highly reliable for diagnostic imaging as early as 10 minutes after injection. This could have important implications for improving workflow and decreasing wait times in Nuclear Medicine Departments compared with more traditional PET agents such as FDG-PET. The results also suggest that FAPI-46 could be an excellent theranostic agent as it binds to its target soon after injection and maintains a high level of uptake over several hours while steadily decreasing background activity.

**KEY POINTS**

**QUESTION:** Tumor residence time of FAP-ligands (FAPI-46) varies in different tumor entities and this investigation explore FAPI-46 from 10 min to 3h post injection in varies cancers.

**PERTINENT FINDINGS:** FAPI-46 is characterized with a rapid and persistent tumor resitence time from 10 min and up to 3h enabling a robust tumor-to-background-ratios (TBR).

**IMPLICATIONS FOR PATIENT CARE:** FAPI-46 describes a rapid tumor uptake in different tumor entities and also tumor retention over 3h post injection, which impact imaging procedures and also possible theranostic application in the future utilisation of FAP-ligands.

**References**


1. LeBleu VS, Kalluri R. A peek into cancer-associated fibroblasts: origins, functions and translational impact. *Dis Model Mech.* 2018;11.

2. Kalluri R. The biology and function of fibroblasts in cancer. *Nat Rev Cancer.* 2016;16.

3. Sahai E, Astsaturov I, Cukierman E, et al. A framework for advancing our understanding of cancer-associated fibroblasts. *Nat Rev Cancer.* 2020;20.

4. Loktev A, Lindner T, Burger EM, et al. Development of Fibroblast Activation Protein-Targeted Radiotracers with Improved Tumor Retention. *J Nucl Med.* 2019;60:1421-1429.

5. Koerber SA, Staudinger F, Kratochwil C, et al. The Role of (68)Ga-FAPI PET/CT for Patients with Malignancies of the Lower Gastrointestinal Tract: First Clinical Experience. *J Nucl Med.* 2020;61:1331-1336.

6. Chen H, Pang Y, Wu J, et al. Comparison of [(68)Ga]Ga-DOTA-FAPI-04 and [(18)F] FDG PET/CT for the diagnosis of primary and metastatic lesions in patients with various types of cancer. *Eur J Nucl Med Mol Imaging.* 2020;47:1820-1832.

7. Kratochwil C, Flechsig P, Lindner T, et al. (68)Ga-FAPI PET/CT: Tracer Uptake in 28 Different Kinds of Cancer. *J Nucl Med.* 2019;60:801-805.

8. Röhrich M, Leitz D, Glatting FM, et al. Fibroblast Activation Protein-Specific PET/CT Imaging in Fibrotic Interstitial Lung Diseases and Lung Cancer: A Translational Exploratory Study. *J Nucl Med.* 2022;63:127-133.

9. Hu K, Wang L, Wu H, et al. [(18)F]FAPI-42 PET imaging in cancer patients: optimal acquisition time, biodistribution, and comparison with [(68)Ga]Ga-FAPI-04. *Eur J Nucl Med Mol Imaging.* 2022 Jul;49:2833-2843.

10. Wang S, Zhou X, Xu X, et al. Dynamic PET/CT Imaging of (68)Ga-FAPI-04 in Chinese Subjects. *Front Oncol.* 2021;11:651005.

11. Ferdinandus J, Kessler L, Hirmas N, et al. Equivalent tumor detection for early and late FAPI-46 PET acquisition. *Eur J Nucl Med Mol Imaging.* 2021;48:3221-3227.

12. Geist BK, Xing H, Wang J, et al. A methodological investigation of healthy tissue, hepatocellular carcinoma, and other lesions with dynamic (68)Ga-FAPI-04 PET/CT imaging. *EJNMMI Phys.* 2021;22:8.

13. Meyer C, Dahlbom M, Lindner T, et al. Radiation Dosimetry and Biodistribution of (68)Ga-FAPI-46 PET Imaging in Cancer Patients. *J Nucl Med.* 2020;61:1171-1177.

14. Glatting FM, Hoppner J, Liew DP, et al. Repetitive early FAPI-PET acquisition comparing FAPI-02, FAPI-46 and FAPI-74: methodological and diagnostic implications for malignant, inflammatory and degenerative lesions. *J Nucl Med.* 2022:26:jnumed.122.264069.

15. Giesel FL, Kratochwil C, Lindner T, et al. (68)Ga-FAPI PET/CT: Biodistribution and Preliminary Dosimetry Estimate of 2 DOTA-Containing FAP-Targeting Agents in Patients with Various Cancers. *J Nucl Med.* 2019;60:386–392.

16. Röhrich M, Naumann P, Giesel FL, et al. Impact of (68)Ga-FAPI PET/CT Imaging on the Therapeutic Management of Primary and Recurrent Pancreatic Ductal Adenocarcinomas. *J Nucl Med.* 2021;62:779-786.

17. Giesel FL, Kratochwil C, Schlittenhardt J, et al. Head-to-head intra-individual comparison of biodistribution and tumor uptake of 68Ga-FAPI and 18F-FDG PET/CT in cancer patients. *Eur J Nucl Med Mol Imaging.* 2021;1-9.

18. Mona CE, Benz MR, Hikmat F, et al. Correlation of 68Ga-FAPi-46 PET Biodistribution with FAP Expression by Immunohistochemistry in Patients with Solid Cancers: Interim Analysis of a Prospective Translational Exploratory Study. *J Nucl Med.* 2022;63:1021-1026.

19. Ferdinandus J, Costa PF, Kessler L, et al. Initial Clinical Experience with 90Y-FAPI-46 Radioligand Therapy for Advanced-Stage Solid Tumors: A Case Series of 9 Patients. *J Nucl Med.* 2022;63:727-734.

20. Kratochwil C, Giesel FL, Rathke H, et al. [153Sm]Samarium-labeled FAPI-46 radioligand therapy in a patient with lung metastases of a sarcoma. *Eur J Nucl Med Mol Imaging.* 2021;48:3011-3013.

**Figure Legends:**

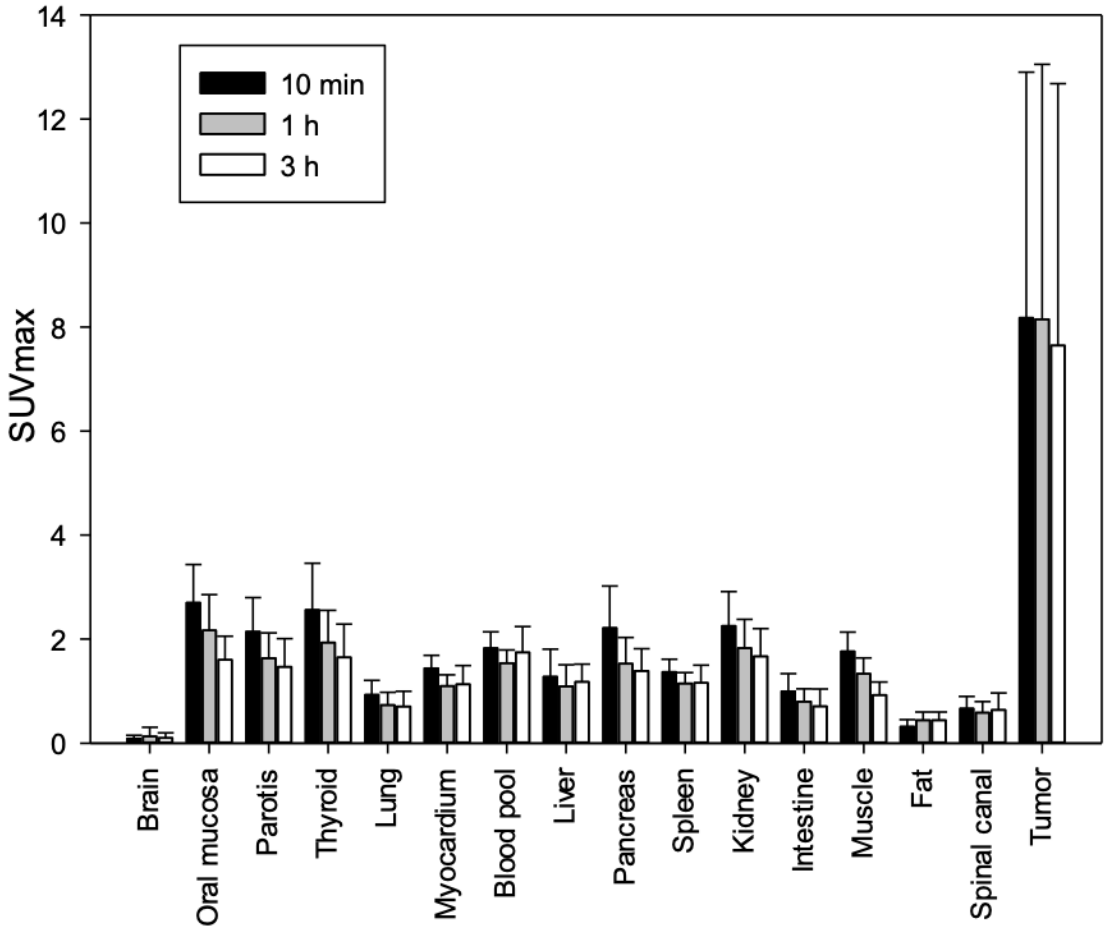


**Fig. 1** Biodistribution SUVmax of FAPI-46 PET at 3 time points in normal organs versus all tumor lesions.

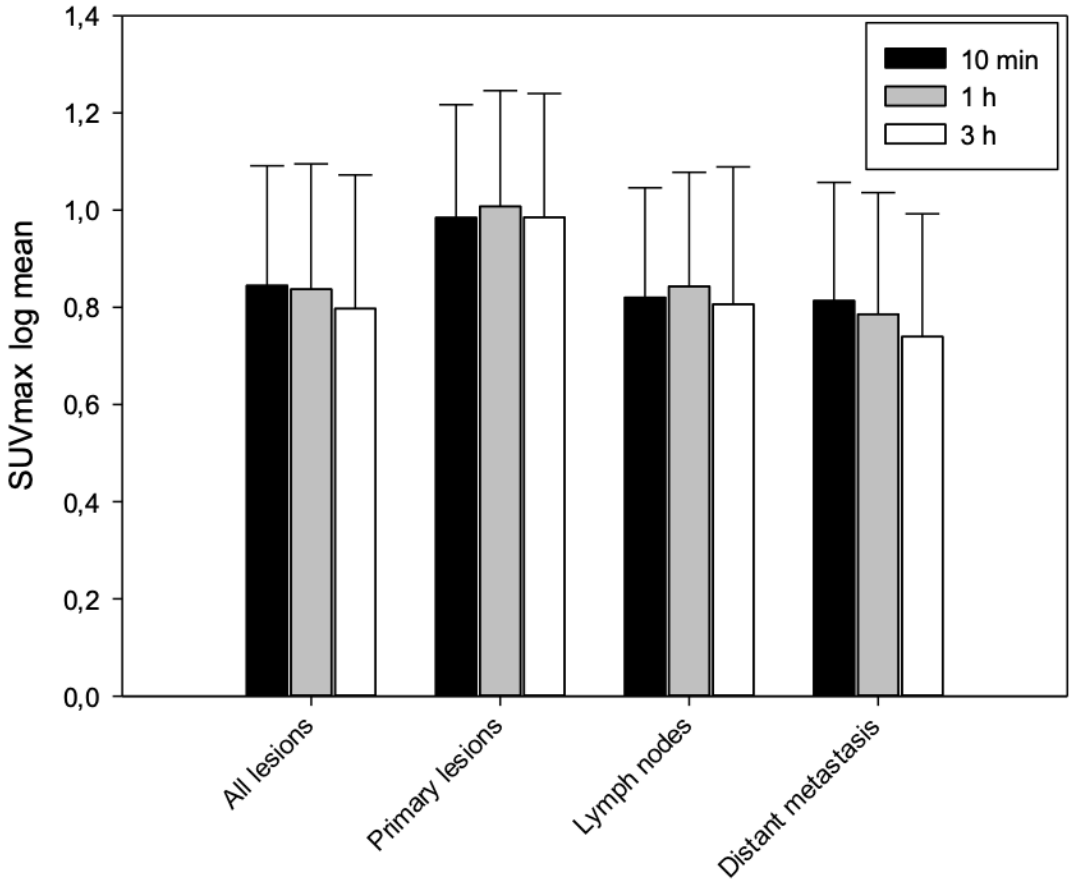


**Fig. 2** Tumor uptake (SUVmax log) through the time points (10 min, 1 h, 3 h) in all lesions (n=171), primary lesions (n=30), lymph node metastases (n=37) and distant metastases (n=104). n: the number of lesions.

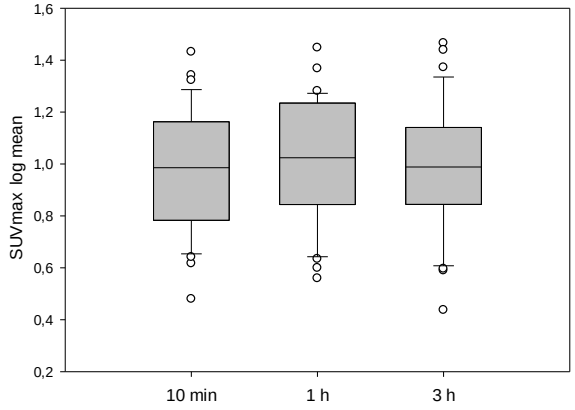


**A**

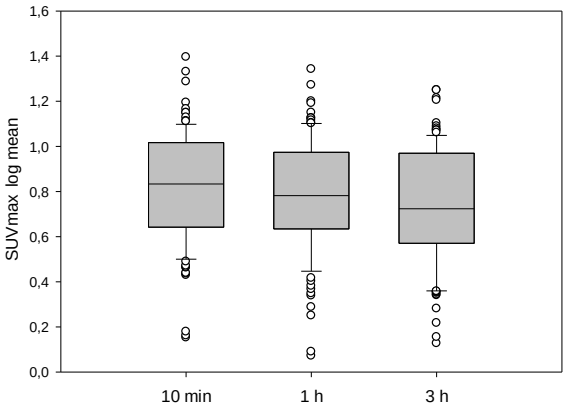


**C**

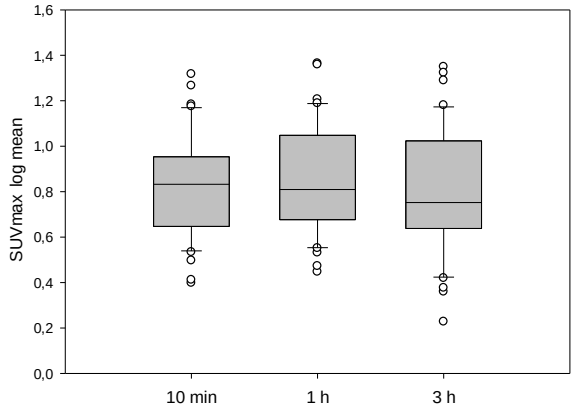


**B**

**Fig. 3** Boxplot. FAPI-46-PET distribution through the time points (10 min, 1 h, 3 h) with tumor uptake (SUVmax log) of (A) primary lesions, (B) lymph node metastases and (C) distant metastases.

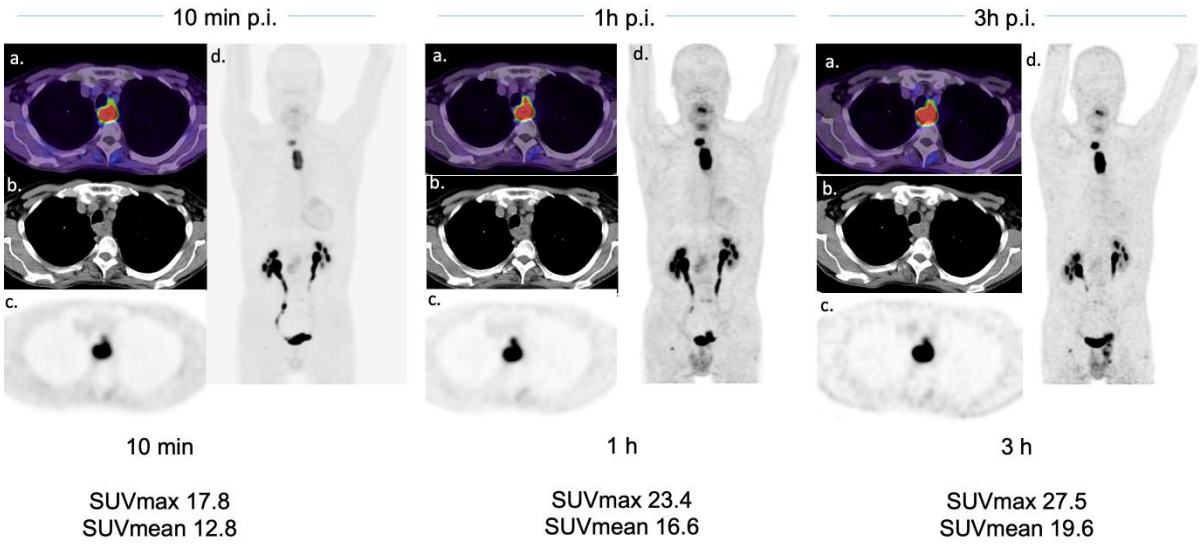


**Fig. 4** This is a case example of a 63 year-old patient with esophageal cancer. FAPI-46 PET/CT was performed for irradiation planning before definitive radiochemotherapy. FAPI-46 PET was performed (10 min, 1 h, 3 h) after injection.

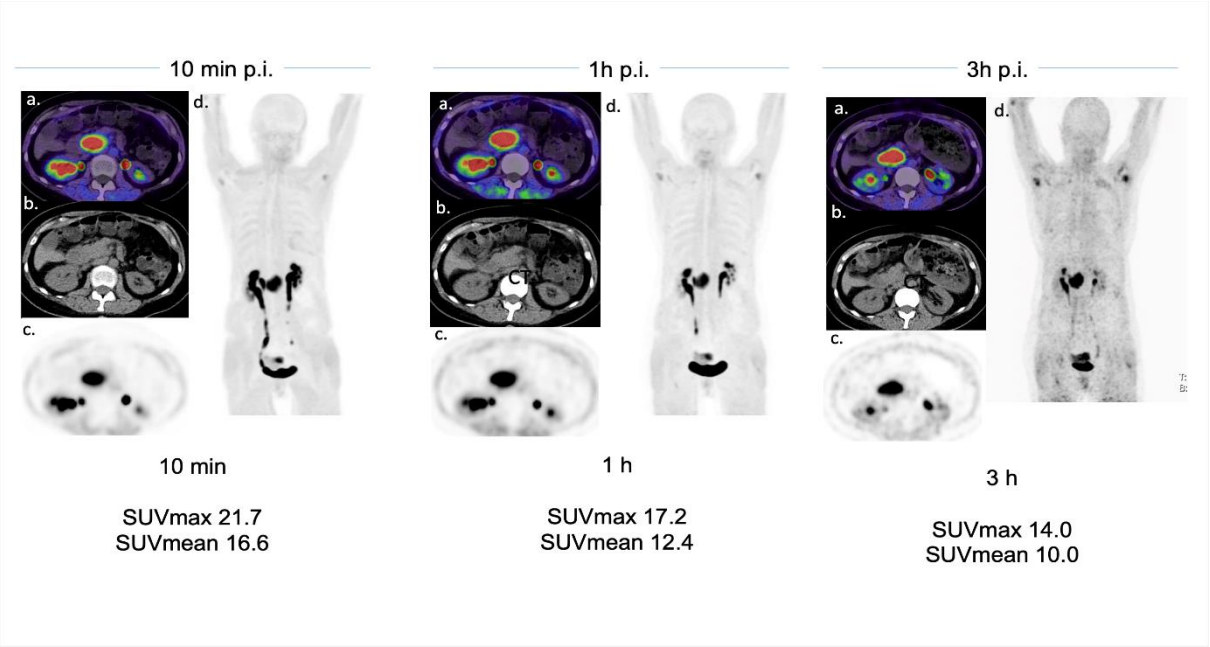


**Fig. 5** This is a case example of a 60 year-old patient with pancreatic cancer. FAPI-46 PET/CT was performed with suspicion of a recurrent mass in the pancreatic head found in ultrasound. FAPI-46 PET was performed (10 min, 1 h, 3 h) after injection.

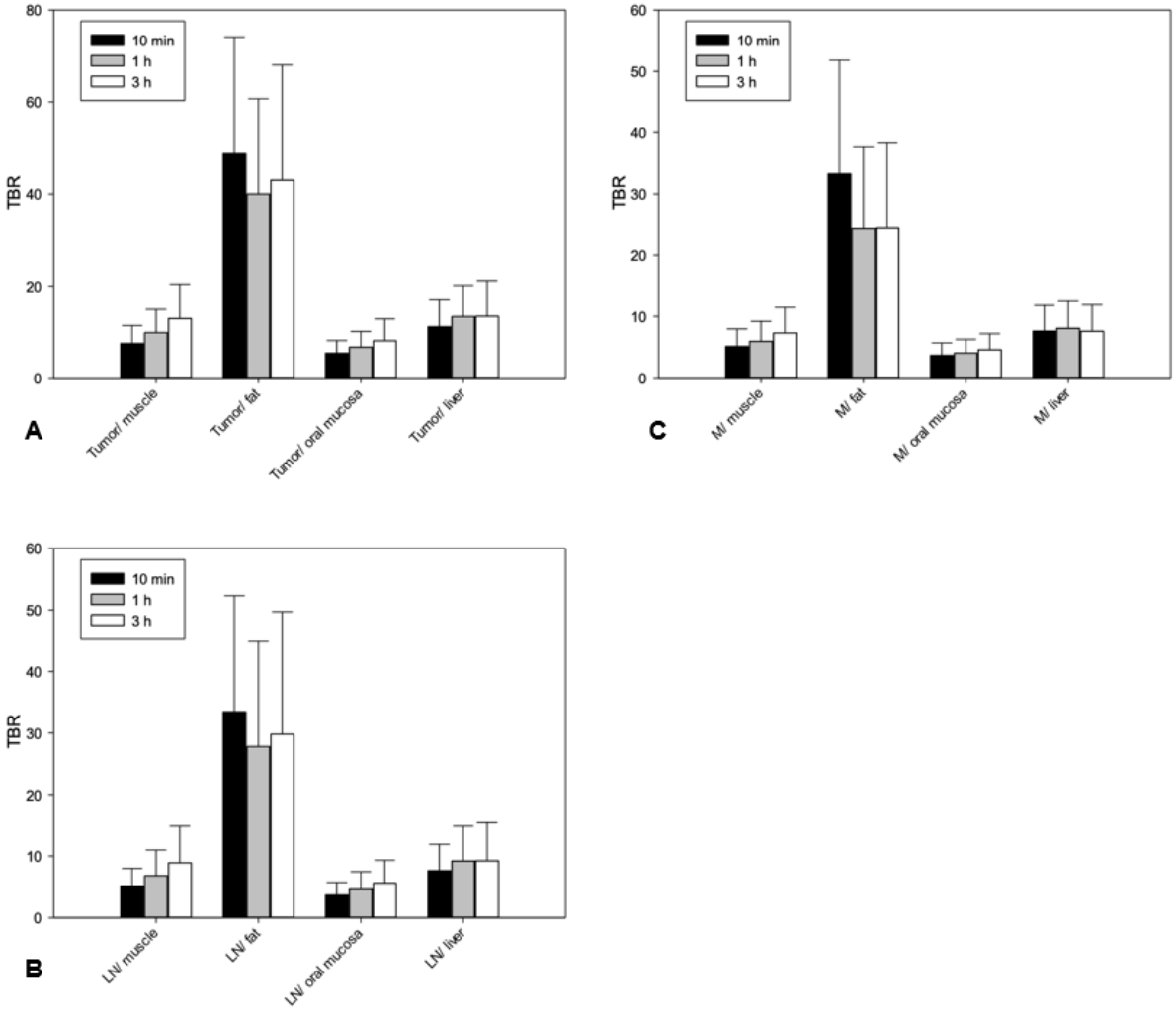


**Fig. 6** TBR through the time points (10 min, 1 h, 3 h) of (A) tumor (primary/relase; n=30), (B) lymph node metastases (n=37) and (C) distant metastases (n=104).

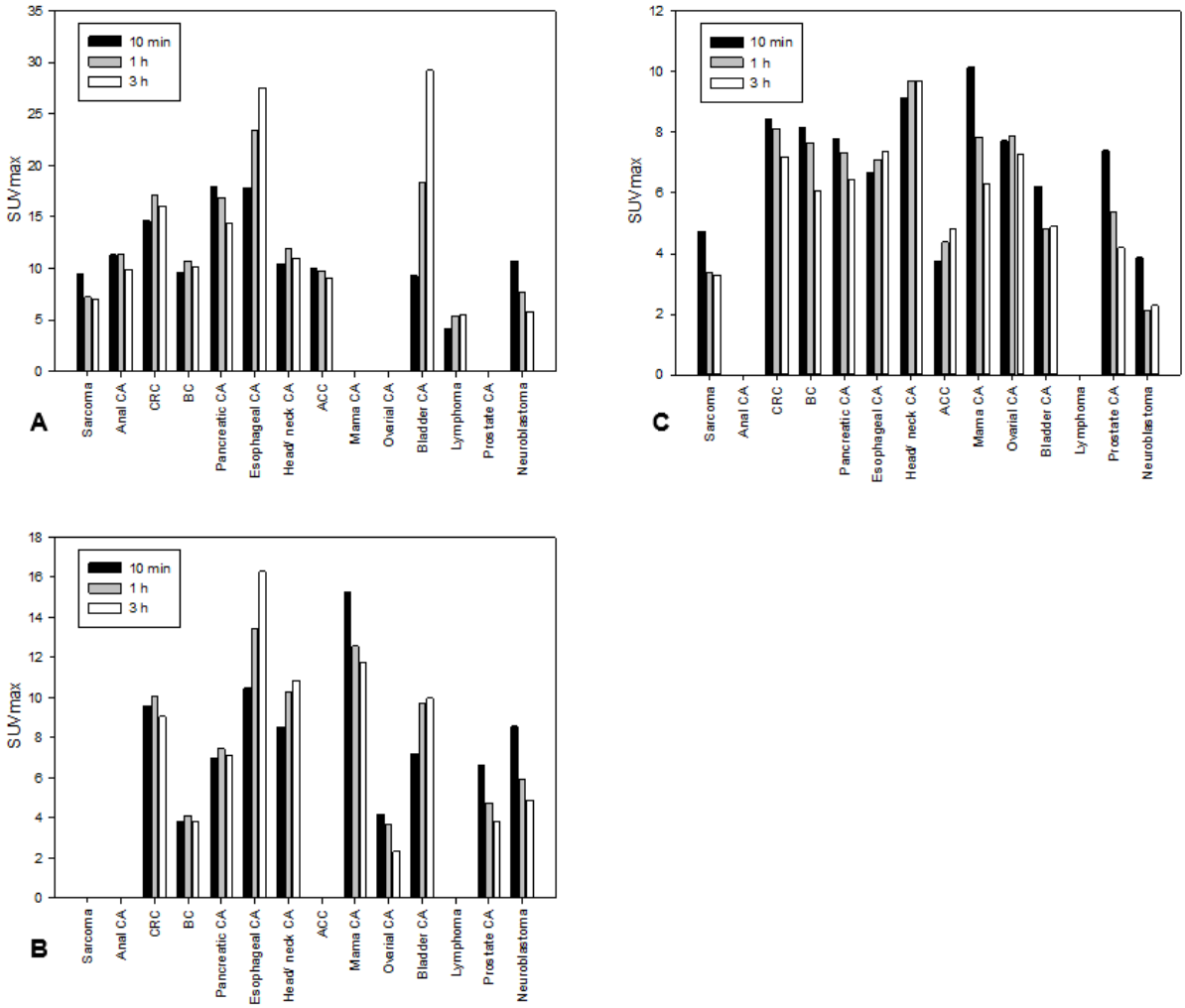


**Fig. 7** Fig. 7 Uptake value of FAPI-46 in various tumor entities. Mean SUVmax of (A) primary/relapse tumors (n=30), (B) lymph node metastases (n=37) and (C) distant metastases (n=104). CA: cancer. CRC: colorectal cancer. BC: bronchial carcinoma. ACC: adrenocortical carcinoma.

**Table 1**: Various Tumor entities in the 43 patients. n: the number of patients with the tumor entity mentioned above.

| Tumor type | n |
|---|---|
| **Sarcoma** | 2 |
| **Anal cancer** | 4 |
| **Colorectal cancer** | 6 |
| **Lung cancer** | 11 |
| **Pancreatic cancer** | 5 |
| **Esophageal cancer** | 2 |
| **Head and neck cancer** | 3 |
| **Adrenocortical carcinoma** | 3 |
| **Breast cancer** | 2 |
| **Ovarian cancer** | 1 |
| **Bladder cancer** | 1 |
| **Lymphoma** | 1 |
| **Prostate cancer** | 1 |
| **Neuroblastoma** | 1 |